

Structural and Thermal Performances of Topological Optimized Masonry Blocks

Gieljan Vantghem^{a,1}, Wouter De Corte^{a,2}, Veerle Boel^{a,3}, Marijke Steeman^{b,4}

GHENT University, Faculty of Engineering and Architecture,

^aDepartment of Structural Engineering, Ghent, Belgium, ^bDepartment of Architecture and Urban Planning,

¹Gieljan.Vantghem@UGent.be, ²Wouter.DeCorte@UGent.be, ³Veerle.Boel@UGent.be,

⁴Marijke.Steeman@UGent.be,

Abstract

Structural topology optimization is the most fundamental form of structural optimization and receives an increasing attention from engineers and structural designers. The method enables the exploration of the general topology and shape of structural elements at an early stage of the design process and gives rise to inspiring and innovative improvements. In this paper, topology optimization as a principle is used to design new types of insulating masonry blocks. Two main objectives are addressed: maximizing the structural stiffness and minimizing the thermal transmittance. The first part of this paper uses these objectives to create new block topologies. A general problem is formulated and the influences of boundary conditions, external loading, and filter value on the resulting geometry are discussed. In general, maximizing the stiffness is in strong contrast to minimizing the thermal transmittance. This causes problems not encountered in conventional topology optimization. Nevertheless, by adjusting the interpolation schemes and adding multiple load groups, convergent solutions are found. An isotropic material model with an enforced solid-or-empty distribution is considered as the primary method. The optimized block topologies are then thoroughly analyzed to review their structural and thermal performance using the commercial finite element software Abaqus. The direct compressive strength of the block is a measure of the structural performance and the equivalent thermal conductivity gives an indication of the thermal performance. The second part then gives some thoughts on three-dimensional optimization and the incorporation of mesostructures in the design.

Keywords: *Topology optimization, Masonry block, Stiffness optimization, Thermal transmittance.*

1. Introduction

Structural topology optimization offers designers and engineers an innovative method to optimize the shape of engineering and architectural structures. It is a mathematical algorithm that, for a given design domain and based on clearly defined boundary conditions, can find the optimal combination of performances such as strength and rigidity, and cost in terms of material consumption. Topology optimization is not new, but in recent years its usage has greatly increased due to the improved accessibility of computational resources and algorithmic efficiency. One of the main reasons why topology optimization is so popular these days is the weight savings it can offer, especially in aerospace and automotive industries.

Many applications already exist, one problem limiting the use of topology optimization is that the resulting optimized shapes often tend to possess a high degree of complexity which makes the production process more difficult and expensive. This is also one of the main reasons why its use in structural engineering or architectural applications is still limited nowadays. This issue is partially being put aside thanks to the rise and the development of new manufacturing processes such as laser sintering, laser melting, and material deposition/extrusion also known as additive layer manufacturing or 3D printing. While most common 3D printers use thermoplastics as printing material, printing with concrete and steel is no longer an idea that only exists in a futuristic mindset. For example, the Chinese company WinSun Decoration Design Engineering Co has 3D printed a full scale building with 3D printing techniques [1] and the Dutch company MX3D has plans for printing the world's first 3D printed steel bridge in Amsterdam in 2017 [2]. The concept for this bridge was inspired by topology optimization.

With the help of topology optimization algorithms, structures and building components can be optimized for more than just strength or rigidity. Other objectives include not only the optimization of buckling loads, adjusting the natural frequencies of a structure, and improving the nonlinear response to a load, but also finding the optimum shape in regards to thermal transmittance or moisture transport. This freedom that topology optimization can offer, is precisely the key reason why its use has become so promising in many industries, including the construction industry.

In the field of modern construction, thermal efficiency has become increasingly important. The progressively strict requirements in terms of energy performance defined by the European Energy Performance of Buildings Directive and the growing interest in energy-neutral buildings has insured that research in this domain is very active [3]. In general, one can say that the energy performance of a building depends upon a large number of aspects. In fact, to many to list

Nomenclature

General symbols

| | |
|----------------------------|---|
| C^T, C^S | thermal and structural objective |
| d | thickness (m) |
| e | element |
| E | Young's modulus (GPa) |
| \mathbf{f} | global load vector |
| \mathbf{K}, \mathbf{K}_e | global and element stiffness or conductivity matrix |
| p | penalization value |
| p_x, p_y | in-plane and out-plane loading |
| q | heat flux (W/m^2) |
| \mathbf{u} | global displacement vector |
| U | thermal transmittance ($\text{W/m}^2 \text{K}$) |
| V_f | available volume (m^3) |

Greek symbols

| | |
|-----------------------------------|---|
| α_i, α_e | Internal and exterior heat transfer coefficients ($\text{W/m}^2\text{K}$) |
| Γ_{si} | warm side of the boundary |
| η | density measure |
| $\theta_i, \theta_e, \theta_{si}$ | inner, outer, and inner surface temperature ($^\circ\text{C}$) |
| $\boldsymbol{\theta}$ | vector of nodal temperatures |
| λ, λ_{eq} | (equivalent) thermal conductivity (W/mK) |
| ρ | material density |
| σ | direct compressive strength (MPa) |
| v | volume (m^3) |
| χ | element variable |
| Ω | design domain |

them all in here. One of the main requirements to improve the energy efficiency of a building is to have an excellent insulation layer between the interior space and the exterior. To accomplish this, masonry blocks with improved thermal conductivity can be used. The book 'Eco-efficient Masonry Bricks and Blocks' by F. Pacheco et al. provides the reader with an up-to-date, state-of-the-art review about eco-efficiency of masonry units, their design, performance, and durability [4]. Pore forming techniques such as the insertion of organic material in fired clay bricks serve a possible solution to increase the thermal resistance. Cellular concrete is another widely used building component that has more or less the same effect. Conversely, this paper focusses on the improvement of the general shape of blocks in order to improve their equivalent thermal conductivity. In other words, the thermal efficiency is being improved by finding the optimum cross-sectional area, independent from the material properties. This in turn can allow the construction of single-leaf masonry walls with high thermal performances.

Insulating masonry blocks already exist in a variety of configurations. Some have multicores, other have interlocking parts. The design of an insulated perforated masonry block is defined based on three main parameters: (1) structural behavior associated to requirements of the construction system, (2) thermal performance, and (3) ergonomics [5]. The structural behavior is primarily defined by the compressive strength of the block, measured both perpendicular and parallel to the mortar bed. Other mechanical parameters such as shear, flexural strength, and robustness to combined vertical and horizontal in-plane loading are also important but exceed the scope of this paper. Of course, the thermal performance also takes a major role in the design of insulated masonry blocks. The geometry and arrangement of the internal cells heavily influence the thermal conductivity coefficient [4]. Large perforations or voids give a significant lower equivalent thermal conductivity, but also make the block weaker. Therefore, it is crucial to find the best possible material arrangement for a fixed material fraction. For fired clay units, further geometric requirements can be found in EC6 which mentions the recommended percentage of holes, the thickness of the webs and shells, and their combined thicknesses [6]. Some of these requirements were adopted by this study but were not considered as mandatory. Finally, concerning ergonomics, attention was given to the ease of use of the masonry blocks, like i.e. easy manually handling.

In this paper, the influence that topology optimization techniques can offer to the design of insulating masonry blocks is addressed. These techniques enable a drift away from traditional optimization methods like parametric studies and allow algorithms to determine the optimum shape of an element, based on clearly defined boundary conditions without prejudice of the engineer - designer. First, the governing equations and different study methods that were used in this paper to determine the structural and thermal performances are given. Next, a general problem is formulated and using two sets of optimized geometries, the results of various topology optimizations are presented and their performances analyzed. Finally, some thoughts on three-dimensional optimization, the further improvement of the topology optimization algorithm and the influence that 3D printing has on the design process are also given.

2. Theoretical background

2.1. Classical topology optimization

This section briefly describes the basic principles of topology optimization and gives an overview of the different objectives as used in this study. The homogenization method described by Bendsøe and Kikuchi [7] and the method of moving asymptotes developed by Svanberg [8] were applied. For an extensive report on the theoretical background of topology optimization the reader is referred to Bendsøe and Sigmund [9].

As previously mentioned, topology optimization renders the optimum distributions of a limited amount of material in the design space in function of a number of pre-defined boundary conditions. The finite element method is used to

discretize the design domain and each element is assigned a unique design variable. This variable can be interpreted as the element density. The value of this variable is located in $[0,1]$ and is coupled with the material properties of the element, such as the Young's modulus or the heat conduction coefficient. After a specific analysis, each of these variables is updated. If an element performs weak towards the imposed objective, its value, the density, is reduced. In the other case, the value is enlarged. By making use of interpolation curves (to be explained further on) the intermediate values are eliminated and thus enforcing a 0-1 (solid or empty) distribution. This isotropic solid or empty (ISE) topology, can then be regarded as a representation of the optimized geometry. The elements with a value almost equal to zero can be considered as cavities and elements with a value equal to 1 represent the solid material.

The most frequently used objective is to maximize the stiffness of a design domain under given conditions (minimum compliance problem) and is described as follows:

$$\begin{aligned} \min C^S(\boldsymbol{\rho}) &= \mathbf{f}^T \mathbf{u} \\ \text{s.t.:} & \sum_{e=1}^{N_e} v_e \rho_e \leq V_f \\ & \rho_e \in [0,1] \quad e = 1, \dots, N_e \\ \text{with:} & \mathbf{K}(\boldsymbol{\rho}) \mathbf{u} = \mathbf{f} \end{aligned} \quad (1)$$

In this equation, C^S is the 'structural' objective function, \mathbf{f} is the external load vector, \mathbf{u} is the displacement vector, v_e is the element volume, ρ_e is the element density, V_f is the accessible volume, and $\mathbf{K}(\boldsymbol{\rho})$ is the global stiffness matrix defined by:

$$\mathbf{K}(\boldsymbol{\rho}) = \sum_{e=1}^{N_e} \left(E_{\min} + \eta_1(\boldsymbol{\rho}) (E_{\max} - E_{\min}) \right) \mathbf{K}_e^0 \quad (2)$$

where \mathbf{K}_e^0 represents the element stiffness matrix corresponding to an element with a Young's modulus of 1 and E_{\min} and E_{\max} have values of the Young's modulus of the element. E_{\min} typically represents the voids, as such a very small but positive number is taken. Whereas E_{\max} takes the value of the reference material. η_1 is the element density measure and is depending on the interpolation scheme (Fig 1). Very often the SIMP interpolation function (Fig. 1a) is applied. In this function the density of the element is raised to the power of p , where p is the penalization factor and is required to be different from 1 to insure an ISE topology. Other interpolation schemes such as RAMP (Fig. 1b) and SINH (Fig. 1c) can also be used.

When the optimized elements should be made of two or more types of material, more design variables can be added. Eq. (3) shows the use of a second element variable χ , which makes it possible to distribute two types of material (i.e. "soft" and "hard" material) and voids (when $\chi=0$). In this equation, E_{\min} represents the voids and takes a very small positive value, the "soft" or the least stiff material is represented by E_{soft} , and the "hard" or stiffest material is represented by E_{hard} .

$$\mathbf{K}(\boldsymbol{\rho}) = \sum_{e=1}^{N_e} \left(E_{\min} + \eta_2(\chi) \left(E_{\text{soft}} + \eta_1(\boldsymbol{\rho}) (E_{\text{hard}} - E_{\text{soft}}) - E_{\min} \right) \right) \mathbf{K}_e^0 \quad (3)$$

As mentioned before, the topology optimization algorithm in this study is also operated with an objective that tries to minimize the thermal transmittance of the design domain. In other words, the equivalent thermal conductivity is being optimized. Consider a two-dimensional rectangular design domain (Ω) where the heat flows from the left side (Γ_{si}) to the right side (Γ_{se}). The top and the bottom of the design domain are adiabatic. The left side is surrounded by air at a temperature θ_i , while the right side is in contact with air at a temperature of θ_e . The heat transfer coefficients α_i and α_e represent the exchange of thermal energy between the body's surface and its surroundings. Under steady-state conditions, the unknown temperature field of the design domain is governed by the well-known heat conduction equation. By measuring the nodal surface temperature on the warm side of the domain (Γ_{si}), the U -factor and the λ -value can in turn be calculated. To adopt this problem into a topology optimization objective, the integral of all inner surface temperatures (θ_{si}) is maximized. This is stated into the following equation:

$$\max C^T(\boldsymbol{\rho}) = \int_{\Gamma_{si}} \theta_{si}(\boldsymbol{\rho}) d\Gamma$$

$$\begin{aligned}
& \text{s.t.:} && \sum_{e=1}^{N_e} v_e \rho_e \geq V_f \\
& && \rho_e \in [0, 1] \quad e = 1, \dots, N_e \\
& \text{with:} && \mathbf{K}(\boldsymbol{\rho}) \boldsymbol{\theta} = \mathbf{f}
\end{aligned} \tag{4}$$

In this equation, C^T is the ‘thermal’ objective, \mathbf{f} is the thermal load vector, $\boldsymbol{\theta}$ is the vector of nodal temperatures, v_e is the element volume, ρ_e is the element density, V_f is the accessible volume, and $\mathbf{K}(\boldsymbol{\rho})$ is the global conductivity matrix defined by:

$$\mathbf{K}(\boldsymbol{\rho}) = \sum_{e=1}^{N_e} \left(\lambda_{\min} + \eta_l(\boldsymbol{\rho}) (\lambda_{\max} - \lambda_{\min}) \right) \mathbf{K}_e^0 \tag{5}$$

Notable in this formulation (Eq. (4)) is that not a maximum, but a minimum volume fraction is imposed. This is reasonable because in order to make the thermal transmittance smaller, as little material as possible is to be used. Subsequently an inverse interpolation function will have better results. For the SIMP-method, it is sufficient to adjust the penalization value by values such as 1/3, 1/4, and 1/5 in stead of 3, 4, and 5 (Fig 1a) whereas for the other interpolation methods, the function itself is adjusted. These inverse functions are rendered by a dashed line (Fig. 1b and 1c).

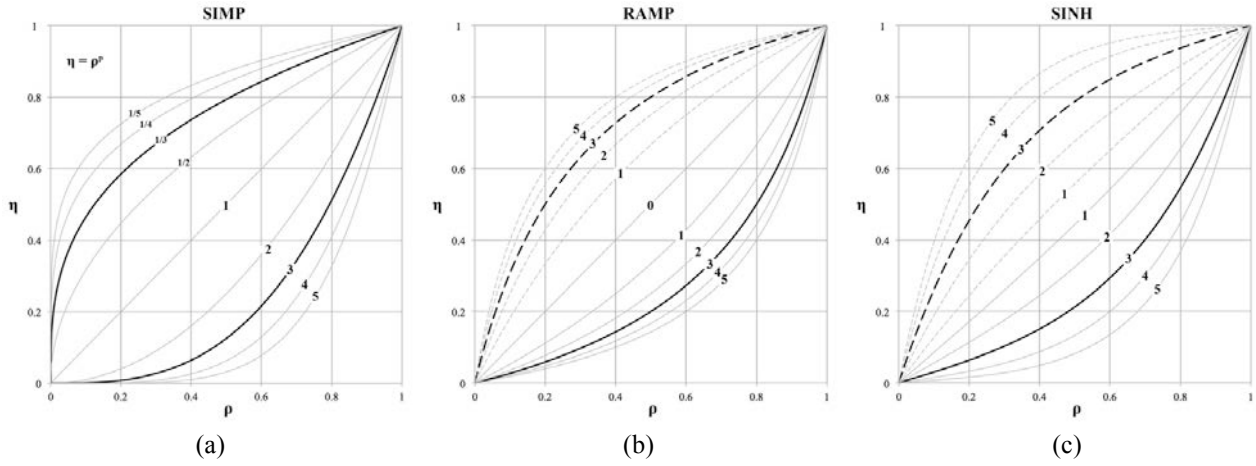


Figure 1. Most widely used interpolation schemes: (a) SIMP ($\eta_{\text{simp}} = \rho^p$), (b) RAMP ($\eta_{\text{ramp}} = \frac{\rho}{1 + p(1 - \rho)}$);

$$(\eta_{\text{ramp}}^{\text{inv}} = 1 - \frac{1 - \rho}{1 + p(1 - \rho)}) \text{ and (c) SINH } (\eta_{\text{sinh}} = \frac{\sinh(p\rho)}{\sinh(p)}); (\eta_{\text{sinh}}^{\text{inv}} = 1 - \frac{\sinh(p(1 - \rho))}{\sinh(p)})$$

2.2 Determination of the structural performance

Typical masonry blocks are built from fired clay or concrete. In both cases the material properties can be seen as heterogeneous and anisotropic. Together with the presence of mortar or grouted joints the structural properties are not straightforward [10]. Besides direct compressive failure, the failure of common masonry blocks is characterized by spalling, buckling, separation of the shells, and vertical splitting and crushing of the webs [5]. An in-depth study regarding the influence of different material properties and highly specific failure modes lays outside the scope of this study. On the other hand, the structural performance has to be studied to some degree. To enable the analysis of the structural efficiency, one specific material model is used for all masonry blocks. This material model was taken from the work of Bolhassani et al. [10], in which the heterogeneous and anisotropic properties of the units and their joints are simulated by an Abaqus compatible concrete damage plasticity model (Fig. 2). Using this model, the nonlinear responses of the masonry units are studied.

2.3 Determination of the thermal performance

To determine the thermal performance of the different blocks, the equivalent thermal conductivity is calculated. The three main types of heat transfer are conduction, radiation and convection. Thermal conduction relates to the transport of heat within a body. The heat will flow from particles with a higher kinetic energy to less energetic particles. The heat flow is dependent on the temperature difference across the thickness and the thermal conductivity of the material (λ). For

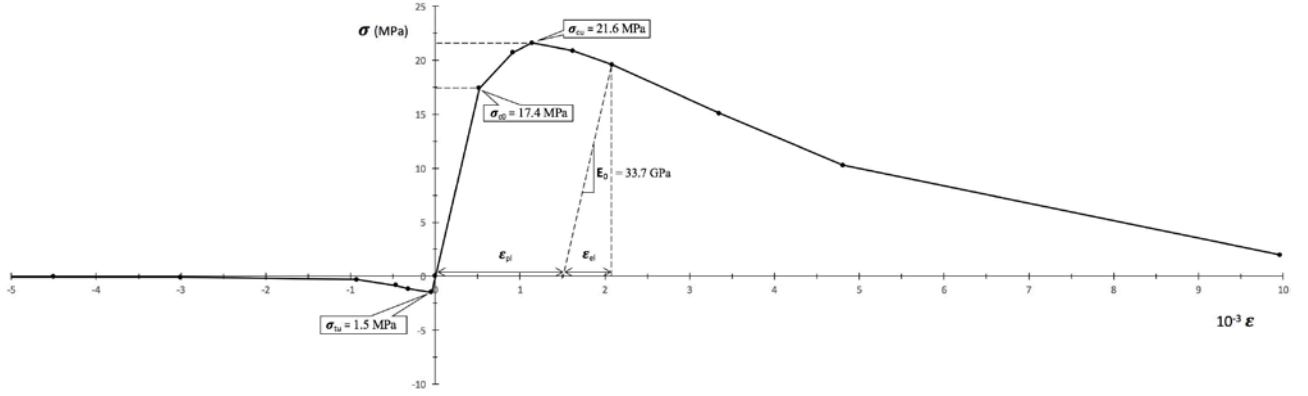


Figure 2. Response of the material to uniaxial loading in tension and compression

the calculations in this paper the λ -value of the solid material is set to 0.28 W/mK and the λ -value of the voids is set to 0.040 W/mK. The exchange of thermal energy between the body's surface and the ambient surroundings is considered a combination of convection and radiation and is expressed by two convective heat transfer coefficients α_i and α_e . Their values are respectively 7.7 W/m²K and 25 W/m²K and indicate the relation between the heat flux (q) and the temperature difference between the surface area (θ_{si}, θ_{se}) and the surrounding temperature (θ_i, θ_e). The values for θ_i and θ_e are respectively 20°C and 0°C. Because it is impossible to directly calculate the equivalent thermal conductivity of the block and the thermal transmittance (U -factor) can not be calculated by simplified methods, the following formula is used:

$$U = \alpha_i \frac{\theta_i - \theta_{si}}{\theta_i - \theta_e} \quad (6)$$

Subsequently, the commercial finite element software Abaqus calculates all unknown nodal surface temperatures (Fig. 3) and determines the weighted average. The formula is adapted into the following:

$$U = \frac{1}{|\Gamma_{si}|} \int_{\Gamma_{si}} \alpha_i \frac{\theta_i - \theta_{si}}{\theta_i - \theta_e} d\Gamma \quad (7)$$

where $|\Gamma_{si}|$ is the length of the inner surface. Finally, with the aid of the calculated U -factor, the equivalent thermal conductivity (λ_{eq}) can be calculated. In Eq. (8), d is the thickness of the block.

$$\lambda_{eq} = \frac{d}{\frac{1}{U} - \frac{1}{\alpha_i} - \frac{1}{\alpha_e}} \quad (8)$$

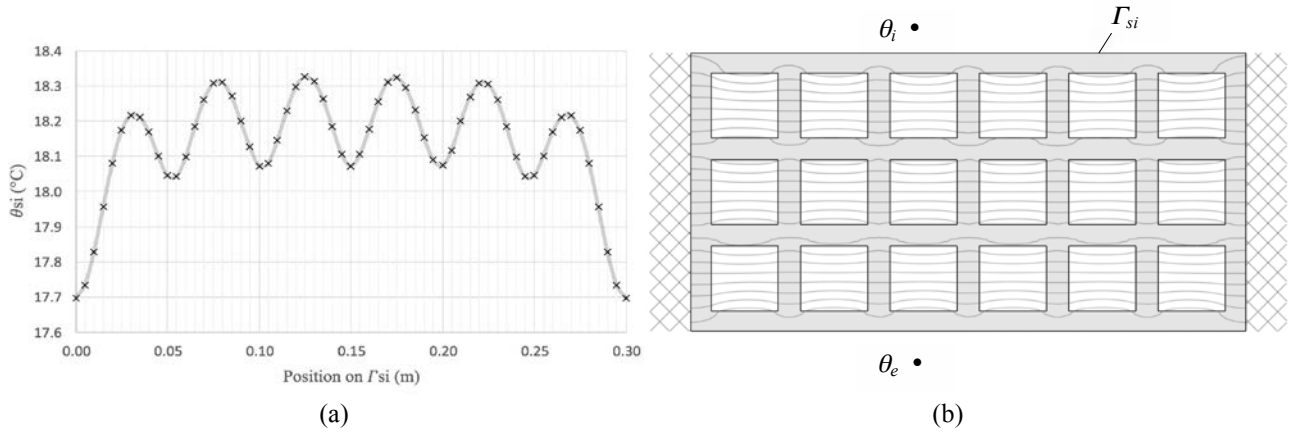


Figure 3. Nodal temperatures on the internal surface (a) of a random insulating masonry block (b)

3. Design of optimal masonry blocks. A two-dimensional case study

3.1. Problem formulation

In this section of the paper, topology optimization is used to improve the cross-sectional surface geometry of masonry blocks. To do this, the optimization algorithms and related objectives discussed in section 2 are applied on a rectangular design domain and the results of two different sets are presented. The aim of this study is to find the best possible material distribution to reduce the thermal transmittance and lower the equivalent thermal conductivity. As is typical in topology optimization problems, the results are strongly dependent on the pre-defined boundary conditions. Therefore, the problem is precisely formulated first.

To start with, a reference block is chosen to enable the comparison of the resulting geometries with a regular masonry block. The design of this block is inspired by an eco-friendly ceramic masonry block. Its dimensions are 300 mm long, 140 mm wide, and 190 mm high (Fig. 4a) and the ratio between the net and the gross volume is exactly 50%. These dimensions and volume ratio are then adopted to construct the design domain of the optimization. When the thermal conductivity coefficients and the convective heat transfer coefficients of section 2.3 are maintained, the equivalent thermal conductivity of this reference block has a value of $\lambda_x=0.121$ W/mK with respect to the x-axis, $\lambda_y=0.127$ W/mK to the y-axis, and $\lambda_z=0.160$ W/mK to the z-axis. The direct compressive strength of this reference block, defined as the maximum load divided by the gross area, is calculated with Abaqus as described in section 2.2, and is evaluated to be 3.5 N/mm^2 in the x-direction, 1.8 N/mm^2 in the y-direction, and 10.5 N/mm^2 in the z-direction.

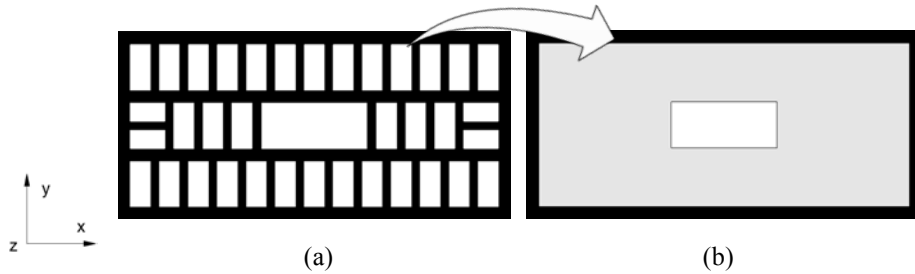


Figure 4. (a) Geometry of the reference masonry block (cross-sectional view) and (b) the design domain of the optimization (the gray area is to be optimized)

The topology optimization problem is studied in two dimensions. This means that only the horizontal cross-sectional area ($300 \times 140 \text{ mm}$) is optimized. As explained in section 2.1, the primary objective will be the minimization of the thermal transmittance of the design domain. When this ‘thermal’ objective (C^T) is the only objective considered, and no other design constraints are active, no useful results are obtained. The optimization algorithm struggles to converge and the material is positioned in random strips in the design domain, as an optimal arrangement is nonexistent (Fig. 5a). This problem is partially resolved by assigning fixed densities to the sides of the block (Fig. 5b). Another, more useful solution is presented by Bruggi and Taliercio [11]. In this paper the in-plane and out-of-plane structural compliances of the blocks are constrained and by doing so, the lateral stiffnesses of the blocks are optimized at the same time. This also makes it possible to include European code requirements concerning minimal strength values. According to Eurocode 8 the minimum value for the direct mean compressive strength in the direction perpendicular and parallel to the mortar bed are respectively 5.0 N/mm^2 and 2.0 N/mm^2 [12]. These conditions are taken into account by assigning two load groups, each having two counteractive uniform loads on the boundary of the design domain (Fig. 5c).

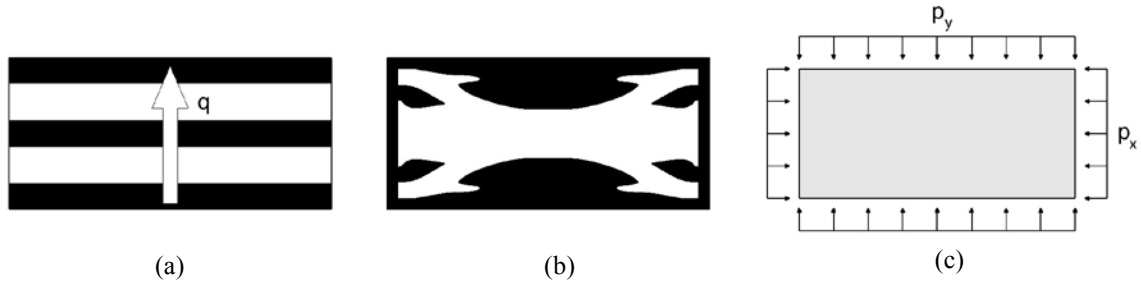


Figure 5. Problem formulation. (a) bar code problem, (b) thermal optimization with a fixed boundary density of 1, and (c) design domain with a uniform loading illustrated

Before the first set of optimized blocks is presented the significant influences of the penalization value, the filter value, geometric restrictions, and external loading are demonstrated. For this particular study the structural compliance problem is used, because this objective is best known in general and is more convenient to operate with. Fig. 6 shows the obtained results. A considerable distinction between the various results is observed: Firstly, Fig. 6a and 6b illustrate the

optimal results in which the stiffness in the y-direction relative to the x-direction is weighted more. Secondly, Fig. 6c and 6d show the results where the stiffness in both directions is considered equally important. Thirdly, the design domains in Fig. 6e and 6f are loaded with concentrated loads instead of uniform loads. Finally, in Fig. 6g and 6h ergonomics is considered by enforcing the appearance of a central void and a minimum web thickness is also imposed by using an appropriate filter value.

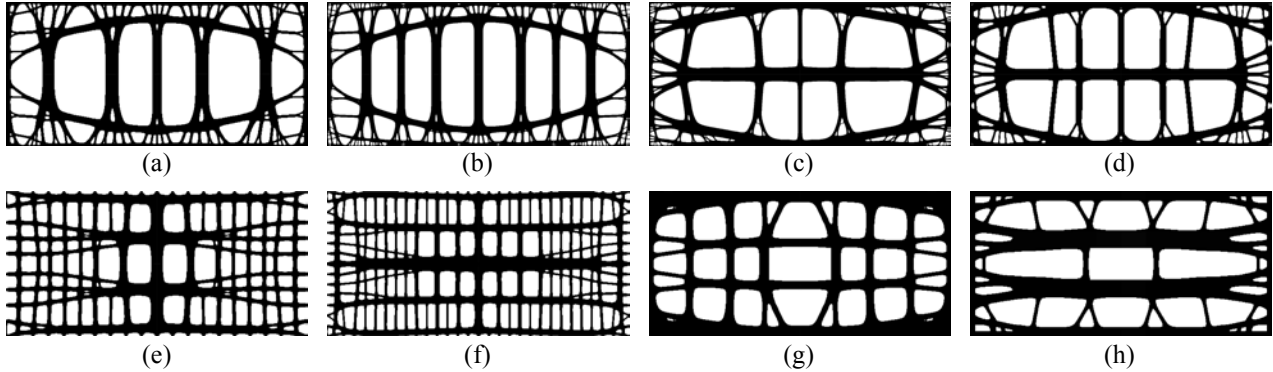


Figure 6. Examples of topological optimized rectangular masonry blocks to illustrate the influences of the penalization value, the filter value, geometric restrictions, and external loading

In these first trials it is found that the penalization value is best to be taken around $p=3$, as it delivers the best results. In addition, in order to prevent the appearance of small webs, the filter value should be in agreement with the mesh size. In what follows, the filter value is assigned the number 6 which means six elements are needed to drift from an element with a density of 1 to an element with a density of 0. When used along side a mesh size of 600 by 280 elements, the minimum web thickness is equal to 3 mm. After a sufficient amount of iterations this value is reduced to 1 to retrieve a clean geometrical boundary. The interpolation function used in set 1 is the SIMP function with a penalization value equal to 3. In the second optimization set, where the ‘thermal’ objective is also considered, the inverse SINH function is added for heat transfer optimizations with a p -value of 4. In all sets (Fig 7 and 8), the elements on the boundary of the block (8 mm wide) have a fixed density of $\rho=1$ and in the center of the design domain, a rectangular zone of approximately 80 by 34 mm, has elements with densities fixed to $\rho=0$ (Fig. 4b). Additionally, all resulting geometries have a volume fraction equal to 50%.

3.2. Optimized masonry blocks. Results

The first set of results demonstrates the influence of the structural compliance (C^S) on the equivalent thermal conductivity and compressive strength of optimized shapes. The optimized geometries are shown in Fig. 7. The masonry block positioned in the middle (Fig. 7c) is optimized with an in-plane (p_x) and out-of-plane (p_y) load ratio equal to one, whereas Fig. 7a and 7b show the resulting geometries for a block with a higher in-plane / out-of-plane load ratio. In contrast, Fig. 7d and 7e have a lower load ratio. The values of thermal and structural performances of these geometries are given in Table. 1 and are compared to the values of the reference block. Numbers typed in bold have a relative better value in comparison to the reference block.

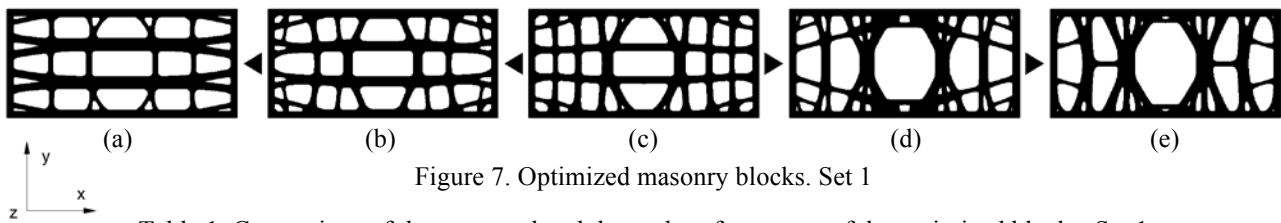


Figure 7. Optimized masonry blocks. Set 1

Table 1. Comparison of the structural and thermal performances of the optimized blocks. Set 1

| Fig. | p_x/p_y | λ_x (W/mK) | λ_y (W/mK) | λ_z (W/mK) | σ_x (kN) | σ_y (kN) | σ_z (kN) |
|------|-----------------|--------------------|--------------------|--------------------|-----------------|-----------------|-----------------|
| 4a | Reference block | 0.121 | 0.127 | 0.140 | 4.4 | 2.1 | 10.5 |
| 7a | 4 | 0.144 | 0.102 | 0.140 | 5.0 | 1.7 | 10.5 |
| 7b | 2 | 0.137 | 0.113 | 0.140 | 3.9 | 1.8 | 10.5 |
| 7c | 1 | 0.127 | 0.125 | 0.140 | 2.9 | 2.6 | 10.5 |
| 7d | 1/2 | 0.120 | 0.131 | 0.140 | 2.9 | 2.9 | 10.5 |
| 7e | 1/4 | 0.112 | 0.137 | 0.140 | 1.9 | 3.1 | 10.5 |

The first thing that can be concluded, is that the higher the load ratio is set, the lower its thermal properties in the y-direction and the better its structural properties in the x-direction are. Additionally, improving the performances in one direction, negatively influences the other direction. Besides these facts, one can presume that for every load ratio studied, and taken into account the predetermined conditions, the optimum material distribution is found. So when the lateral stiffnesses of the block are to be as big as possible, these topologies tend already towards thermally-efficient material usage. Nevertheless, in common practice, the value of the volume fraction is mostly determined by the minimum vertical compressive strength of the block. This means that the lateral stiffnesses of masonry blocks do not have to be maxed out. Once the required values have reached their minima, the positioning of the excess material becomes important. Therefore, a second optimization set is studied.

The second set of results (Fig. 8) shows the optimal topologies of masonry blocks in which the structural stiffnesses are gradually reduced from left to right while minimizing the thermal transmittance across the y-direction. The minimization of the equivalent thermal conductivity is considered as the primarily objective (C^T) and the lateral stiffnesses are constrained. In Fig. 8a both the thermal and structural objective are enabled to measure the value of the in-plane and out-of-plane stiffnesses of the initial design. In the optimizations that follow, the structural objective is then replaced by a similar stiffness constraint that is some factor larger than its initial value. Fig. 8b and 8c show the resulting geometries in which the values of the stiffnesses were decreased by respectively a factor 2 and 4. Fig. 8c shows an optimized topology in which no lateral stiffnesses were required. Table. 2 gives the values of thermal and structural performances of these geometries in comparison to the values of the reference block. Again, numbers that are presented in bold have a relative better value in comparison to the reference block.

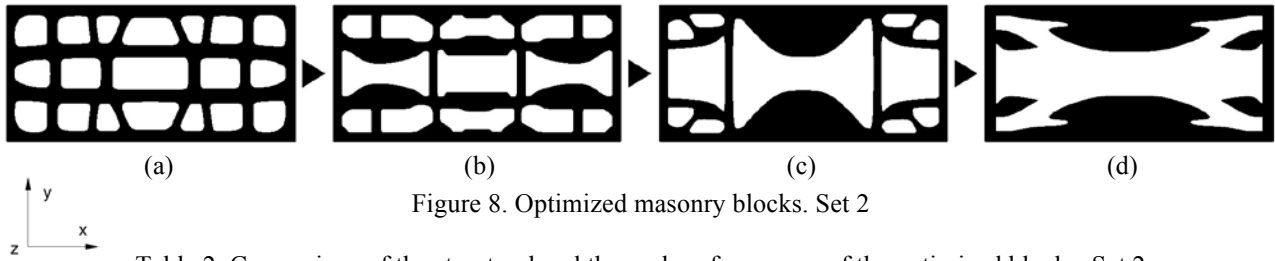


Table 2. Comparison of the structural and thermal performances of the optimized blocks. Set 2

| Fig. | Reduction of initial stiffness | λ_x (W/mK) | λ_y (W/mK) | λ_z (W/mK) | σ_x (kN) | σ_y (kN) | σ_z (kN) |
|------|--------------------------------|--------------------|--------------------|--------------------|-----------------|-----------------|-----------------|
| 4a | Reference block | 0.121 | 0.127 | 0.140 | 4.4 | 2.1 | 10.5 |
| 8a | 1 | 0.136 | 0.116 | 0.140 | 4.5 | 2.5 | 10.5 |
| 8b | 2 | 0.139 | 0.099 | 0.140 | 3.7 | 1.7 | 10.5 |
| 8c | 4 | 0.129 | 0.099 | 0.140 | 2.1 | 1.7 | 10.5 |
| 8d | 10000 | 0.130 | 0.086 | 0.140 | 1.8 | 1.1 | 10.5 |

The first thing that can be observed is that decreasing the required lateral stiffnesses of the block has a positive effect on the equivalent thermal conductivity, but negatively influences the compressive strength. Nevertheless, when considering the minimum values presented by EC 8 (see section 3.1) the lateral stiffness in the x-direction of block 8c is still sufficient. Secondly, block 8a seems to improve the structural performance, as well as the thermal performance relative to the reference block. Considering its topology is very similar to Fig. 7c, and yet the performances are not exactly what you would call the same, some thoughts must be given to the effectiveness of the optimization algorithm when only linear elastic material is considered. The inclusion of nonlinear material models into the algorithm could overcome this inaccuracy.

4. Thoughts on three-dimensional optimization and incorporation of mesostructures in the design

4.1 Optimization in the third dimension

This study has mainly focused on a two-dimensional optimization and the reason why optimization in the third dimension is not studied in this paper is twofold: Firstly, most of the existing masonry blocks are characterized as being two-dimensionally extruded and only a different production process could change this. Nonetheless, the introduction of this paper mentions the rise of new production techniques, such as additive manufacturing, so the search for optimal shapes should not be limited by these current manufacturing methods. The second, more decisive reason that limits this study to two-dimensions, is that according to the used study methods, three-dimensional topology optimization will not provide any additional information. It is found that for a topology optimization in three dimensions where displacement-controlled loadings are applied in the z-direction, only extruded two-dimensional shapes are created. In contrast, force-controlled

loadings enable the redistribution of material in the z-direction as well. Even though these loadings represent in a lesser way real loading situations, an example of a three-dimensional optimization is shown in Fig. 9. Another way three-dimensional topology optimization could further improve the shape of masonry blocks is when the optimization of nonlinear failure modes such as buckling and spalling of the vertical webs could be added to the optimization algorithm. This way, narrow webs could be reinforced by adding horizontal spacers.



Figure 9. A three-dimensionally optimized masonry block cut in half through the midsection (X-Y plane)

4.2 Incorporation of mesostructures

In the previously mentioned optimization studies, ISE topologies were always enforced upon the optimized geometries. As explained by Bendsøe and Kikuchi, for structural topology optimization, this is justified when the SIMP interpolation function is used, since a physical representation of these intermediated densities exist [9]. In the thermal optimization algorithm, inverse interpolation functions were created to aid the iteration process and removal of these intermediated densities, but no physical representation of these densities exist. Therefore, another possibility is to allow intermediated densities to remain active and replace these regions by mesostructures. Such mesostructures or lattice structures could then be designed to have good thermal as well as structural properties. A combined hybrid optimization approach where topology optimization techniques and the formation of regions with intermediated densities is illustrated on Fig. 10. In this study concentrated loads are applied instead of uniform loads. Another technique in which multiple density regions could be created, would be the use of multi-material optimization algorithms as described in section 2.1.

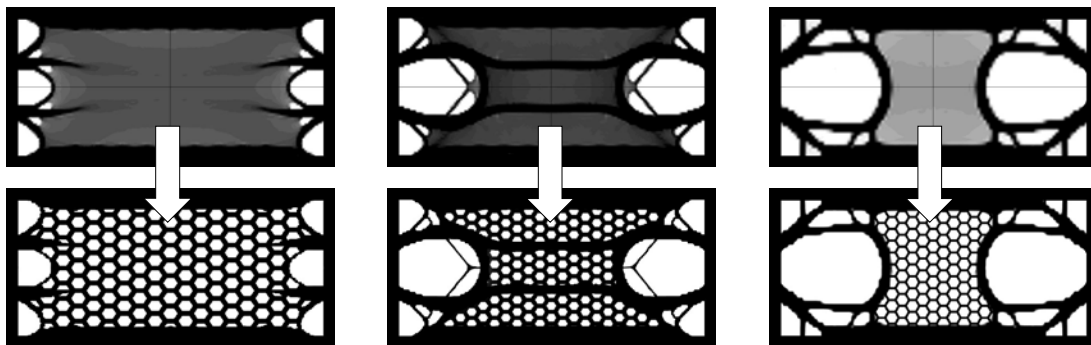


Figure 10. Adaption of the intermediate densities of topology optimization

5. Concluding remarks. Future perspectives

In this paper an advanced understanding of the basic principles of topology optimization and the value of combined physics optimizations is illustrated. Different objectives were used to design new shapes for insulating masonry blocks. Unlike traditional optimization methods such as sizing optimization and shape parameterization methods, it is the optimization algorithm that determines the optimal shape of a construction element without prejudice of the engineer - designer. Therefore, topology optimization can give a clue to why certain geometries are preferred and can in turn inspire the designer early on in the design process. Additionally, when clearly defined boundary conditions are chosen, optimum shapes can be found. Using topology optimization as a design tool does not mean that traditional optimization methods should be abandoned, but it offers another approach on which new ideas and concepts can develop. Finding the most optimal design is not straightforward since attention must be given to the problem formulation in a way that global maxima can be found. Essential in this paper is that the classical structural topology optimization was extended to an approach in which structural and thermal aspects were combined, which is something that should be considered more often in design. The inclusion of moisture transport and thermal mass optimization could further add to the value of the calculation. In conclusion, in this paper, attempts were made to explore some new ideas and open the existing mindset to thinking beyond the box.

References

- [1] B. Severson, "Shanghai-based WinSun 3D Prints 6-Story Apartment Building and an Incredible Home", 3DPrint.com, 2015. [Online]. Available: <http://3dprint.com/38144/3d-printed-apartment-building/>. [Accessed: 29-Mar- 2016].
- [2] "Dutch startup plans first 3D printed steel bridge to span Amsterdam canal", the Guardian, 2015. [Online]. Available: <http://www.theguardian.com/technology/2015/jun/17/dutch-startup-plans-first-3d-printed-steel-bridge-to-span-amsterdam-canal>. [Accessed: 29- Mar- 2016].
- [3] "Concerted Action | Energy Performance of Buildings Directive", Epbd-ca.eu, 2016. [Online]. Available: <http://www.epbd-ca.eu>. [Accessed: 29- Mar- 2016].
- [4] F. Torgal, Eco-efficient masonry bricks and blocks. Cambridge: Woodhead Pub., 2015.
- [5] P. Lourenço and G. Vasconcelos, "The design and performance of high-performance perforated fired masonry bricks", in Eco-efficient Masonry Bricks and Blocks, 1st ed., F. Torgal, Ed. Cambridge: Woodhead, 2015, pp. 13-41.
- [6] CEN. Eurocode 6: Design of masonry structures - Part 1-1: General rules for reinforced and unreinforced masonry structures. European standard EN 1996-1-1:2006: Brussels: Comité Européen de Normalisation; 2006.
- [7] M. Bendsøe and N. Kikuchi, "Generating optimal topologies in structural design using a homogenization method", Comput Method Appl M, vol. 71, no. 2, pp. 197-224, 1988.
- [8] K. Svanberg, "The method of moving asymptotes—a new method for structural optimization", Int J Numer Meth Eng, vol. 24, no. 2, pp. 359-373, 1987.
- [9] M. Bendsøe and O. Sigmund, Topology optimization. Berlin: Springer, 2003.
- [10] M. Bolhassani, A. Hamid, A. Lau and F. Moon, "Simplified micro modeling of partially grouted masonry assemblages", Constr and Build Mater, vol. 83, pp. 159-173, 2015.
- [11] M. Bruggi and A. Taliercio, "Design of masonry blocks with enhanced thermomechanical performances by topology optimization", Constr Build Mater, vol. 48, pp. 424-433, 2013.
- [12] CEN. Eurocode 8: Design of structures for earthquake resistance - Part 1: General rules, seismic actions and rules for buildings (+ AC:2009). European standard EN 1998-1:2014: Brussels: Comité Européen de Normalisation; 2014.